STUDY OF GAS–SOLID FLOW IN A MULTICHANNEL CYCLONE

Pranas Baltrėnas[1], **Petras Vaitiekūnas**[2], **Inga Jakštonienė**[3], **Simona Konoverskytė**[4]

Department of Environmental Protection, Vilnius Gediminas Technical University,
Saulėtekio al. 11, LT-10223 Vilnius, Lithuania
E-mail: [1]pbalt@vgtu.lt; [2]vaitiek@.vgtu.lt; [3]ingajakstoniene@gmail.com (corresponding author);
[4]saimutmis@gmail.com

Abstract. This paper aims to analyse the problem of the gas–solid particle (SP) flow in the multichannel cyclone (three rings) with tangential inlet (KDG – equipment for separation of solid particles from gaseous fluid flow). It provides a review of experimental and theoretical papers that describe cyclones with a very complex swirling flow. The paper describes the experimental study and numerical modelling of the flow in the multichannel cyclone, the height of which is 0.72 m and the diameter – 0.50 m; with the height of the cylindrical part amounting to 0.29 m, the height of the conical part – 0.43 m, and the inlet area – 0.29×0.034 m^2. The multi-functional measuring instrument Testo 400, intended for measuring the flow velocity in the inlet and outlet of the multichannel cyclone was used in experimental studies of the cyclone. Three-dimensional transport differential equations (Reynolds) for incompressible turbulent flow inside a cyclone are solved numerically using finite volume-based numerical method and turbulence models, namely the Standard k-ε model, the RNG k-ε model.

According to results obtained during the experiments with quartz sand and quartz sand dust pollutants, the highest SP treatment efficiency as regards these pollutants, reaching 85.8–90.4%, was obtained. Modelling results obtained from the numerical tests with the inlet velocity of 6.27–10.78 m/s and, the flow rate of 0.111–0.190 m^3/s have demonstrated a reasonable agreement with experimental and theoretical results. The average relative error was ± 4.3%.

Keywords: multichannel cyclone, solid particles, numerical modelling, turbulence, airflow, one-phase, two-phase flow.

1. Introduction

Cyclones are widely used in oil and recycling industries to separate particles from fluids. This can be explained by the fact that cyclones are easy to use, and they do not require heavy construction, exploitation, maintenance and energy consumption expenses. The use of appropriate materials and construction methods enables scientists to exploit cyclones in high temperature and high pressure when in energy and recycling industries, the use of very efficient equipment can influence such processes as pressurized fluidised-bed combustion (PFBC), integrated gasification combined cycle (IGCC) and fluidised catalytic cracking (FCC). In these processes, cyclones are now almost the only fully-commercial method to separate particles from high-temperature gases (Zhou, Sao 1990; Hu *et al.* 2005; Gujun *et al.* 2008).

Cyclones are defined as funnel-shaped industrial inertial equipment. They are very popular because of simplicity; besides, they are compact and cheap to produce; they have no moving parts and do not require much maintenance. (Boysan *et al.* 1982; Bernardo *et al.* 2006; Jakštonienė, Vaitiekūnas 2009).

Tangential inlet allows separating particles from gases (Altmeyer *et al* 2004, Kaya, Karagoz 2008). They are called inverse conical flow (ICF) cyclones (Derksen 2003). A spiral in the tangential inlet cyclones was modified, which is very effective in separating solid particles from the contaminated gas stream (Hashremi 2006), in which analysis (experiment and modelling) of two types of cyclones was made: ICF cyclone and a modified spiral in the ICF cyclone.

Computational fluid dynamics (CFD) has a great potential to predict the sediments in water (Vaikasas 2010), the flow-field characteristics (Petraitis, Vasarevičius 2001; Braduliene, Vasarevičius 2010), particle trajectories (Baltrenas *et al*. 2008) and the pressure drop in cyclones (Gimbun *et al*. 2005).

Insufficient understanding of the process of two-phase flow in a cyclone does not allow improving its exploitation. Such inadequate understanding arises due to the fact that despite the supposed simplicity, dynamics of flows in cyclones is very complex and includes features such as swirling movement and in certain cases – several reverse-flow circular zones. Theories of closed swirling flow have not yet succeeded in distinguishing many characteristics of the analysed flow. The problem of mathematical modelling of the detailed flow structure includes the solution of closely related non-linear partial differential equations of mass and impulse conservation and has no analytical solution. Besides, discontinuation of turbulence based on the assumption of isotropy (e.g. the k-ε model) cannot be used for strongly swirling flows (Boysan *et al* 1982, Bernardo *et al* 2006). Hoffmann and Stein (2002) claim that the standard k-ε model has its disadvantages when used for strongly swirling flows.

Meier and Mori (1999) provided timely-averaged Navier-Stokes equations for the gaseous phase and related them to the anisotropic turbulence model in combination with the *k-ε* model and algebraic stress equations. After this innovative work, several studies aimed to model turbulence in order to better foresee velocity and pressure. All these studies accepted axial symmetry that allows using two-dimensional model where the solid phase almost does not contact the gaseous field.

Bernardo *et al.* (2006) used a specific turbulence model, known as the Reynolds stress model (RSM), to find certain values for Reynolds stress terms. This model is based on transport equations for all Reynolds stress tensor components and dissipation velocity. RSM provides anisotropic turbulence to flows; when the hypothesis of turbulent viscosity is used, model gives isotropic turbulence. In the first case, Reynolds stress transfer equations are being solved for separate stress components.

Wang *et al.* (2006) applied Reynolds stress model in order to model gas flow in the Lapple cyclone. RSM very precisely predicts swirling flow features, axial velocity, tangential velocity and pressure loss in the model of a cyclone (Sommerfeld 2003; Gujun *et al.* 2008). The following mathematical model can be drawn for this case:

$$\frac{Du}{Dt} = \rho F_i - \frac{\partial p}{\partial x_i} + \frac{\partial}{\partial x_j}\left(\mu \frac{\partial u_i}{\partial x_j} - \overline{\rho u_i' u_j'} \right), \qquad (1)$$

$i, j = 1, 2, 3$. Terms in the (1)-type equations $\overline{\rho u_i' u_j'}$ are called turbulent or Reynolds stresses that require additional differential equations. For this purpose, Reynolds stress equations are used. These equations for the two-dimensional problem are described in the Kavaliauskas and Vaitiekūnas (2001) study. RSM (Reynolds stress model) can reasonably predict swirling flows (Gujun *et al.* 2008). The probabilistic Lagrange model is used in order to model the flow of particles.

Recently pervasive are the cross-type cyclones – centrifugal filters – (Balan *et al.* 2009; Serebrianskij, Novakovskij 2009), the efficiency of which depends on the number of channels.

The aim of this work is to investigate the experiment and numerical modelling of the multichannel cyclone. For this purpose, three-dimensional transport equations with the standard *k-ε* and RNG *k-ε* turbulence model were used.

2. Analysis methods

2.1. Experimental analysis method

The experimental research using the multichannel cyclone was carried out in the Scientific Environmental Technology Laboratory of Vilnius Gediminas Technical University.

The schematic diagram of experimental set-up is presented in Fig. 1. The cyclone was filled with experimental dust using a dust nozzle and dispersed with the help of compressed air pressure (8 bars). Air was blown to the cyclone system using a channel ventilator (1). Tes-

to 400 (2) was used to measure an airflow velocity at the inlet and outlet of the multichannel cyclone. In order to minimise the sampling error occurring due to the formation of a swirling flow in cyclone's outlet, which may first throw particles to external walls, a lattice is fitted inside a pipe in the cyclone's outlet (3). Measurements were carried out using the optical dust concentration monitor *Microdust pro (Casela)* (4).
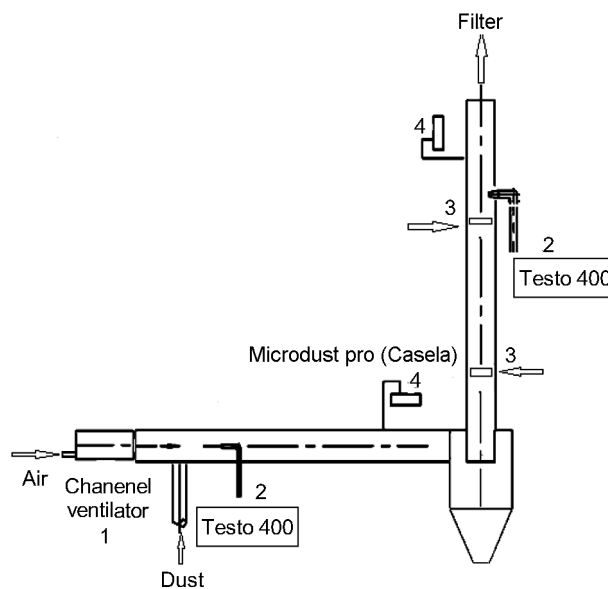

Fig. 1. The schematic diagram of experimental set-up:
1 – channel ventilator, 2 – multifunctional meter Testo 400, 3 – lattice, 4 – dust concentration monitor Microdust pro (Casela)

It is designed for assessing the concentration of solid particles. Its operation is based on the measurement of the angle of scatter of infrared light of 880 nm wavelength spreading in the air polluted with particulates. The monitor consists of: a sampling probe fitted with an infrared light, measurement slot, a light collector, an infrared ray detector; an indicator with analytical signal intensification, processing and representation system, a control button and a liquid crystal display. The main functions of the dust concentration monitor: identification, calculation and indication of solid particles concentration; verification of the technical condition and indication of a liquid crystal display; verification of the condition of a power battery (indication in segments); graphic representation of dust concentration measurement; sensitivity coordination with known concentrations in optical filters from an instrument kit; identification of initial measurement zero (0.0 mg/m^3) concentration point.

Materials used for the preparation of a pollution source: quartz sand (physical density 3200 kg/m^3, particle size 50–400 µm), quartz sand dust (crystalline silicon dioxide) (physical density 2450 kg/m^3, particle diameter 10–100 µm), calcium carbonate (CaCO$_3$) (physical density 2 700 kg/m^3, particle diameter 5–100 µm), which must be dry during measurement. All materials were dried at a temperature of 80 ºC, and after-wards stored at a temperature of 24–26 ºC for 24 hours. Humidity of the particles may not exceed 5%. During the experiment the ambient

temperature varied from 24.4 °C to 25.9 °C, and relative humidity of air reached 58%. Control samples for inlet dust concentrations were supplied to the multichannel cyclone at the fixed time.

Upon completion of each dust measurement and prior to measuring particles of another material, hoses of the aspiration system are cleaned by blowing a strong airflow through them. Each material for the dusty airflow was drawn at a rate of 20 *l*/min. The optical dust concentration monitor Microdust pro (Casela) must be calibrated anew by setting it in a conditional zero position (Baltrėnas, Kvasauskas 2005).

During the experiments air enters the cyclone system via a tangential inlet and airflow velocity is measured in the inlet and outlet with the instrument Testo 400.

A place for flow velocity measurement is selected in the linear section of the air pipe with the settled gas flow in the cyclone. The air pipe section must be free of any obstacles to the flow (valves, bends, ventilators) in 5–6 D (air pipe diameter) up to the measurement point and in 3–4 D behind the measurement point.

To make measurements in the air pipe, holes are bored in the selected place and metal connecting pipes, 40–50 mm long, with screw caps are welded, or openings, 20–30 mm in diameter, are made.

The multifunctional meter Testo 400 is used to determine dimension readings, i.e. m/s, showing an airflow velocity. When parameters of the multifunctional measuring instrument Testo 400 are set, the Pitot tube is placed into the air pipe in which the end of the tube is directed against a gas flow and the tube is slowly pulled from the inner side of the tube towards the middle and backwards. Measurements are started and the average of readings is calculated. Analysis in each point was made three times and the average airflow velocity was calculated.

Principle scheme of the multichannel cyclone. A cyclone consists of two main parts (Fig. 2): cylindrical part (diameter (D_1) – 0.5 m, height (H_1) – 0.29 m), height of the conical part (H_2) – 0.43 m, base diameter (D_2) – 0.16 m, downward (for solid particles, diameter (D_3) – 0.10 m, general cyclone height (H) – 0.72 m. In the cylindrical part fitted there are three different centrifugal radius semicircle 0.29 m in width, which consists of four channels (Fig. 3).

When compared to usual centrifugal air-cleaning equipment, the multichannel cyclone cleans fine solid particles with centrifugal force and filtration, performed in curvilinear channels (7) that have spaces between the rings of channels (3). These spaces divide flow into two parts: larger particles enter the channel of larger radius (6) and fall into the hopper, finer particles are filtered through the air-flow and enter the channel of smaller radius. Cleaned air outflows through the outlet.

2.2. Governing equations and solution method

Turbulent flows are very complex. This is clearly seen in the increased complexity of turbulent velocity equations (such as 1) where additional terms (Reynolds stresses) are used. When modelling these terms, we try to provide
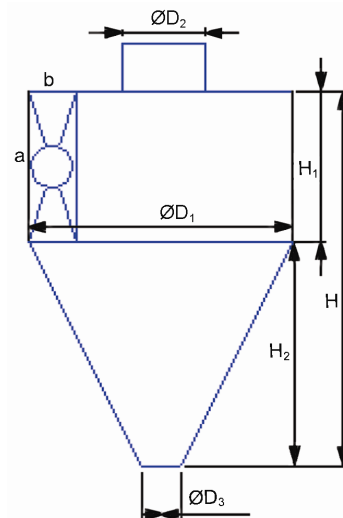

Fig. 2. The multichannel cyclone geometric: inlet (of cylindrical part, inflow cross-section area (a×b) is 0.29×0.034 m^2). Two outlets: downwards (D_3) – for solid particles, diameter 0.10 m; a tube at the top (D_2) – for cleaned air, diameter 0.16 m
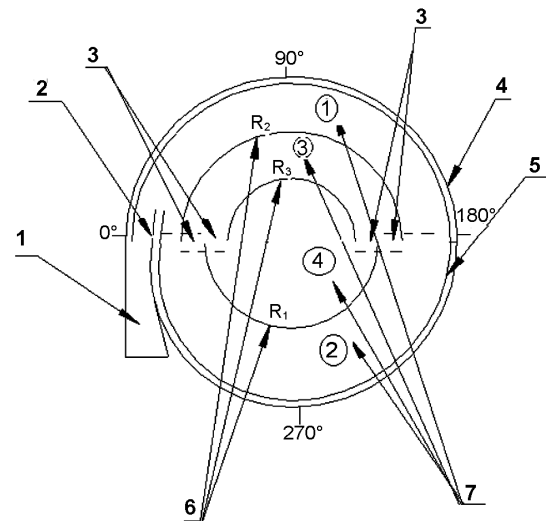

Fig. 3. Scheme of the multichannel cyclone inside (outlook from the top): 1 – inlet for polluted air, 2 – partitions, 3 – spaces between curvilinear rings of various radius, 4 – separation chamber, 5 – circular gap, 6 – rings of various radius (R_1 – 130.7 mm, R_2 – 166.3 mm, R_3 – 95 mm), 7 – curvilinear channels (1, 2, 3, 4)

simple connections as the finite equation form that is solved numerically (simplification of the full equations). This means that the accuracy of the mathematical model that describes flow can be reduced (Vaitiekūnas 1998). The use of the hypothesis of turbulent viscosity allows forming the following differential transport equations (for air flow only):

$$\frac{\partial}{\partial t}(\rho\Phi) + \text{div}(\rho \mathbf{V}\Phi - \Gamma_\Phi \mathbf{grad}\Phi) = S_\Phi, \quad (2)$$

where: t – time; ρ – density; Φ – dependent variable, as a moment to the unit of mass, turbulence energy, its dissipation rate; when $\Phi = 1$ – continuity equation; $\bar{\mathbf{v}}$ – velocity vector; Γ – exchange coefficient of the variable Φ;

S_Φ – flow (source) term to variable Φ. Exchange coefficient for the turbulent flow can be written as:

$$\Gamma_\phi = \rho\,(\nu_l + \nu_t), \qquad (3)$$

where ν_l – molecular coefficient of kinematic viscosity; ν_t – coefficient of turbulent viscosity. The turbulent viscosity μ_T or ν_T can be computed by combining the turbulent kinetic energy k and its dissipation rate ε as follows:

$$\mu_T = C_\mu \rho \frac{k^2}{\varepsilon}. \qquad (4)$$

Transport equations for variables k and ε in the RNG k-ε model, which is derived from Navier-Stokes equations using the renormalisation group theory (Yakhot, Orszag 1986) can be written as:

$$\rho \frac{Dk}{Dt} = \frac{\partial}{\partial x_i}\left(a_k \mu_{eff} \frac{\partial k}{\partial x_i}\right) + G_k - \rho\varepsilon, \qquad (5)$$

$$\rho \frac{D\varepsilon}{Dt} = \frac{\partial}{\partial x_i}\left(a_k \mu_{eff} \frac{\partial k}{\partial x_i}\right) + C_{1\varepsilon}\frac{\varepsilon}{k}G_k - C_{2\varepsilon}\rho\frac{\varepsilon^2}{k} - R. \qquad (6)$$

Unlike the standard k-ε model, this model includes analytical expressions in addition to having an extra term R in the second equation. The model constants are assumed to have the following values: $C_{1\varepsilon}=1.42$, $C_{2\varepsilon}=1.68$ and $C_\mu=0.0845$, $\mathrm{Pr}_{k,T}=\mathrm{Pr}_{\varepsilon,T}=0.7194$.

These governing equations are solved numerically using the finite volume-based method (Spalding 2002; Patankar 1980). According to the basic idea of this method, the computational domain is divided into a number of cells, and differential equations are integrated over each cell using the theorem of divergence (the Gaus–Ostrogradski theorem) to obtain algebraic equations. These algebraic equations are solved iteratively to obtain the field distribution of dependent variables.

Numerical modelling was performed with a numerical calculation grid where the cyclonic area is a three-dimensional space in the cylindrical coordinate system that is divided into cells *x, y, z* directions, x is angle in radians (Bernardo *et al.* 2005).

Governing equations were solved numerically using the finite volume-based method. The use of CFD when modelling flow in cyclones is the best decision as this method is more universal. The use of the optimum modelling scheme CFD allows recording complex flow–particle interaction with a great accuracy (Youngmin *et al.* 1999).

In general, the cellular region of a cyclone is formed of $x \times y \times z = 40 \times 36 \times 45 = 64800$ (Fig. 4) volume cells. These are control velocity cells where velocity components, pressure and turbulent characteristics in radial, tangential and axial directions are calculated.

Airflow velocity at the cyclone inlet is assumed to be uniformed and reaches 6.27–10.78 m/s. The outflow boundary condition was used at the exit. At the walls, the law of flow-solid wall adhesion was applied for velocity, and near-wall treatment was achieved using the standard and non-equilibrium wall functions.
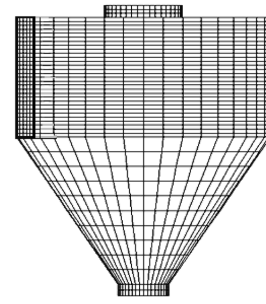

Fig. 4. The multichannel cyclone outline of a calculation grid

3. Results and analysis

3.1. Experimental results

Experimental results were obtained when inlet air–solid flow rate is: 0.111; 0.143; 0.166 and 0.190 m³/s.

Solid particle (SP) concentrations in incoming and outgoing air–dust flow from the KDG cyclone were determined by the spectrometric technique. This technique was employed to measure the concentrations of quartz sand and quartz sand dust in the flows incoming to and outgoing from the KDG cyclone. Data received from spectrometric measurements are presented in Figs. 5 and 6.
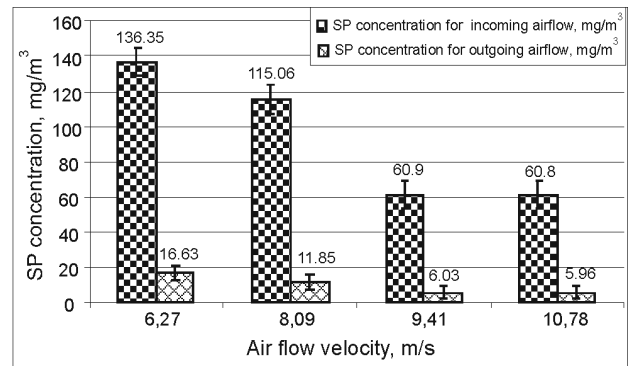

Fig. 5. Dependence of quartz sand SP concentration treatment on air-solid flow velocity in the KDG cyclone with the following SP concentrations for incoming flow (6.27; 8.09; 9.41; 10.78 m/s): 1) 136.35; 2) 115.06; 3) 60.9; 4) 60.8 mg/m³
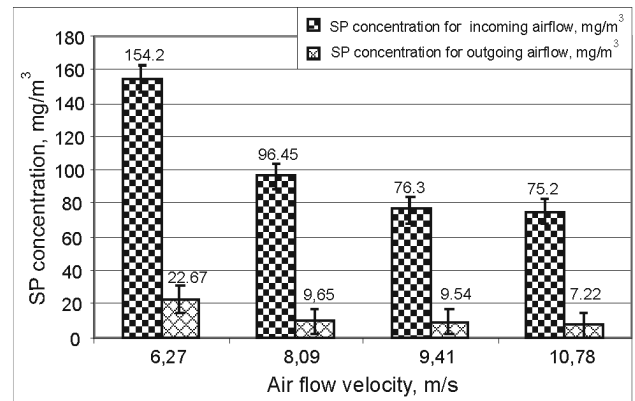

Fig. 6. Dependence of quartz sand dust SP concentration treatment on air-solid flow velocity in the KDG cyclone with the following SP concentrations for incoming flow (6.27; 8.09; 9.41; 10.78 m/s): 1) 154.20; 2) 96.45; 3) 76.30; 4) 75.20 mg/m³

Graphic representation shows the solid particle concentrations determined by the spectrometric technique in the airflow outgoing from the KDG cyclone when air was cleaned from quartz sand and quartz sand dust by changing the operation parameters of the device, i.e. supplied airflow velocity and time of inlet dust concentration. 4 positions of airflow velocity values were set: 6.27; 8.09; 9.41; 10.78 m/s. Time of inlet dust concentration: 50 s for quartz sand, 25 s for quartz sand dust (Figs. 5 and 6).

Figs. 5 and 6 show the dependences of the treatment of SP concentrations determined by the spectrometric technique on airflow velocity (on inflow into the KDG cyclone) when air is cleaned from quartz sand and quartz sand dust with the following initial concentrations: 136.35; 115.06; 60.9; 60.8 mg/m^3 for quartz sand, and 154.20; 96.45; 76.30, 75.20 mg/m^3 for quartz sand dust.

As Figs. 5 and 6 show, with a gradual increase of velocity of the airflow passed through the KDG cyclone (from 6.27 to 10.78 m/s), the treatment efficiency of solid particle concentrations gradually increases: initially (at a velocity of 6.27 m/s) air is cleaned from 136.35 mg/m^3 quartz sand and 154.20 mg/m^3 quartz sand dust up to the concentration of 16.63 and 22.67 mg/m^3, respectively; but when an airflow velocity reaches 4.50 m/s, the concentration of solid particles decreases by around 2.8 and 3.1 times, respectively. Such a decrease in SP concentration testifies to a high treatment efficiency of the air treatment device – the KDG cyclone.

Below are presented the dependences of the treatment of SP concentrations determined during experiments on airflow velocity (on inflow into the KDG cyclone) when air is cleaned from quartz sand and quartz sand dust. The efficiency of cyclone was analysed at the four inflow velocities (see Figs. 5 and 6).

According to results obtained during the experiments with quartz sand and quartz sand dust pollutants, the highest SP treatment efficiency as regards these pollutants, reaching 85.8–90.4%, was obtained.
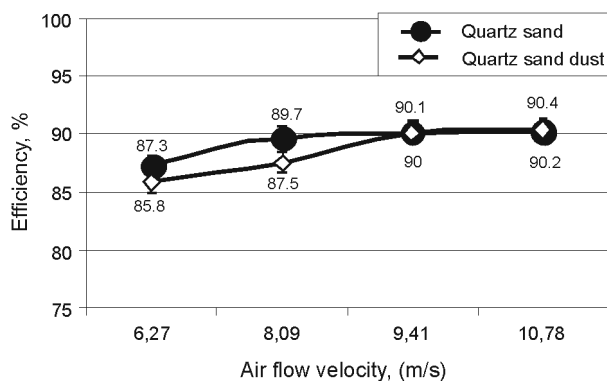
Fig. 7. Dependence of SP concentration treatment efficiency on air-solid flow velocity when air is cleaned from quartz sand and quartz sand dust in the KDG cyclone

As Fig. 7 shows, with a gradual increase of velocity of the airflow passed through KDG cyclone (from 6.27 to 10.78 m/s) treatment efficiency increases; however, at a velocity of 9.41–10.78 m/s the efficiency remains stable reaching around 90.3±0.15%.

3.2. Modelling results and analysis

After taking account of the dimensions of the multichannel cyclone structure (see Figs. 2 and 3), aero-dynamic processes – transport of the inlet airflow velocity in the gas flow at the inlet velocity of 6.27–10.78 m/s within an air pipe – were modelled.

Fig. 8 shows the inflow of the airflow supplied through the multichannel cyclone's inlet, which is within the entire height of a cylindrical part of the cyclone, to the circular part of the cyclone (between cyclone's body and ring R2, Fig. 3). An airflow is supplied to the KDG cyclone via the channel (1) and (2), afterwards the enters channel (3) and finally enters the channel (4), from which the flow splits into two parts: part of the flow enters the channel (3), another – ascends in the channel (4) via the cylindrical part of the cyclone's body to the top towards the airflow outlet.

Having passed through openings intended for solid particle falling into a hopper in the conical part of the cyclone, located by the cyclone body, the flow causes a complicated movement (Fig. 8). Velocity vectors by cyclone walls, as presented in Fig. 8, show movement of the turbulent airflow in the KDG cyclone.

The obtained field of velocity vectors in the KDG cyclone is presented in Fig. 9, where the centre axle of the plane is the top of the cyclone's cylindrical part, i.e. the outlet for the cyclone (exit air pipe).
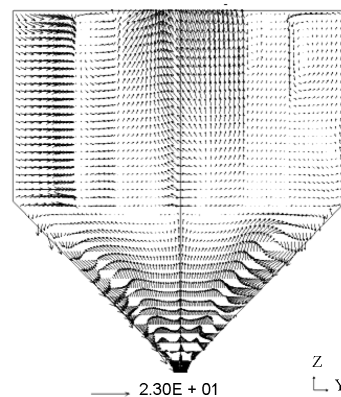
Fig. 8. Field of air flow velocity vectors in the vertical plane of a multichannel cyclone. Scale of velocity vectors is 23.0 m/s
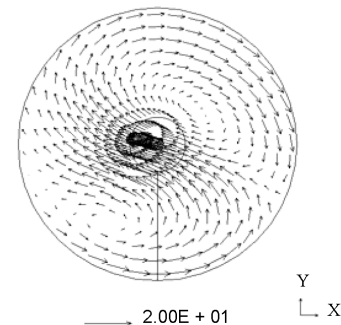
Fig. 9. Field of air flow velocity vectors in the centre axle (outlet) of a multichannel cyclone, scale of velocity vectors is 20 m/s (outlet for cyclone, $D_2 = 0.16$ m)

Fig. 10 shows the projections of the tangential velocity component to z coordinate in the vertical plane of the KDG cyclone. In Fig. 10 and Fig. 11 – velocity vectors with inlet velocity 6.27 and 10.78 m/s.

Comparison between numerical and experimental data results where measurements were made at two points of the KDG cyclone: point No. 1 – at the first ring R_1; point No. 2 – at the second ring R_2 of tangential velocities profiles 0.14 m from No. 2: x = 270°, y = 12 cm) in the KDG cyclone. The results obtained are presented in the Fig 12. It gives a comparison between numerical and experimental results of tangential velocities at the axial position of the top of the cyclone (z = 0.14 m) at the first ring R_1 (point No. 1: x = 90°, y = 9.3 cm) and the second ring R_2 (point No. 2: x = 270°, y = 12 cm) in the KDG cyclone. The results obtained are presented in the Fig. 12. Comparison is undertaken of numerical and experimental results of tangential velocities at the axial position of z = 0.14 m from the top of the KDG cyclone.
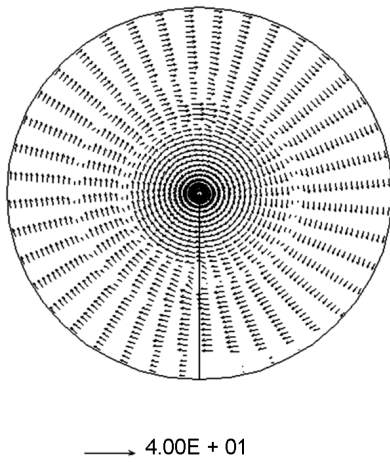

Fig. 10. Field of air flow velocity vectors in the centre axle of a multichannel cyclone, scale of velocity vectors is 40 m/s, in plane z = const 0.15 m from top of the cyclone Uin = 6.27 m/s, D_1= 0.50 m
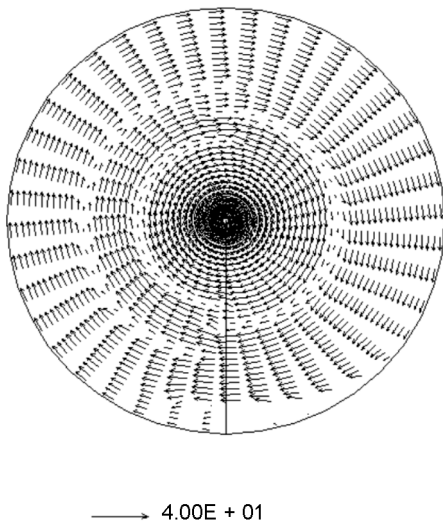

Fig. 11. Field of air flow velocity vectors in the centre axle of a multichannel cyclone, scale of velocity vectors is 40 m/s, in plane z = const 0.15 m from top of the cyclone Uin = 10.78 m/s, D_1 = 0.50 m
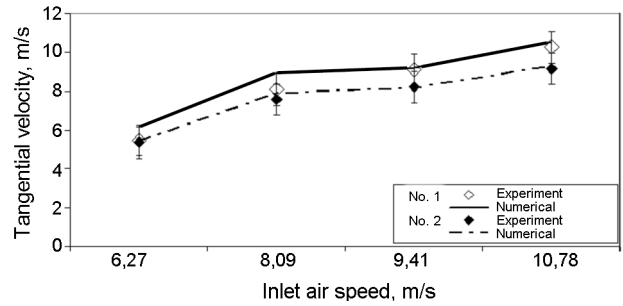

Fig. 12. Comparison between numerical tangential air flow velocity on horizontal plane 0.14 m from the top of the KDG cyclone and experimental data (inlet velocity 6.27, 8.09, 9.41 and 10.78 m/s)

A comparison of experimental and numerical data shows that the numerical results of tangential velocity at the first ring in cyclone (z = 0.14 m, x = 90°, y = 9.3 cm), when the number of cyclone cells is 97200, nearly coincide with the experimental data; and the average relative error is 6.8%. The best agreement of the experimental and numerical data was obtained from the centre of cyclone towards the second ring (x = 270°, y = 12 cm), in which case the average relative error reached 1.8%.

These results were obtained by applying a one-phase RNG turbulence model, which showed a reasonable agreement between experimental and numerical results. The modelling results of aerodynamic processes allow a conclusion that the values measured during airflow velocity investigations within the error limits corresponded to the tangential velocities determined during modelling, the total relative error of which reached 4.3% as in (Vaitiekunas *et al.* 2010).

Turbulent flow inside a tangential inlet cyclone was solved numerically using the CFD method with three different turbulence models, namely the standard *k-ε*, the RNG *k-ε* turbulence model with non-equilibrium wall function and the RSM model. The received numerical results were compared with theoretical (Kaya, Karagoz 2008) and (Bernardo *et al.* 2006), as well as experimental (Patterson, Munz 1996, Cristea *et al.* 1996) data.

The complicated swirling turbulent flow in a cyclone places great demands on the numerical methods and turbulence models employed in the CFD codes when modelling the cyclone pressure drop, as well as axial and tangential velocities (Hoekstra *et al.* 1999; Ingham, Ma 2002).

Although literature widely analyses and describes turbulent transport models of various complexity used in numerical researches, it is not yet clear which of them are the most appropriate for mixed convection.

Researchers Kaya and Karagoz (2008) analysed the performance of various numerical methods and interpolation schemes when studying strongly swirling flows inside a tangential inlet cyclone and compared predictable results with experimental data and numerical values by Gong and Wang (2004).

Comparison of axial and tangential velocity profiles computed using three turbulence models with experimental (Gong, Wang 2004) data is shown that the RSM

turbulence model gives more coincident results than other turbulence models when comparing experimental data.

Although the tendency and behaviour of the theoretical velocity profiles are consistent with experimental data, there are some discrepancies, especially in the core part, when comparing the measured velocities from the literature and the RSM predictions. When this swirling flow is strongly affected by the flow and geometric conditions, and it is difficult to measure velocities precisely in such a complex flow, the conclusion can be made that these discrepancies are due to not only turbulence models and numerical methods, but also experimental and measurement errors. The highly rotating fluid flow generates strong anisotropy in the turbulent structure. This causes the standard k-ε and the RNG k-ε turbulence models to provide inaccurate predictions for the fluid flow. Although the RNG k-ε model gives slightly better results when compared to the standard k-ε model, it fails to provide Rankin-type velocity distributions due to its swirl. Besides, the standard k-ε and the RNG k-ε turbulence models predict the pressure drop. However, the best prediction of the pressure drop is given by the RSM model. This is also confirmed by the modelling results of the work (Kaya, Karagoz 2008).

4. Conclusions

1. Efficiency of the multichannel cyclone (KDG) at the investigated gas-solid flow velocities of 6.27–10.78 m/s was increasing in an asymptotic manner; however, a still higher increase in velocity could produce an inverse effect – either decreased or stable treatment efficiency.

2. The optimum inflow velocity (gas–solid flow) of the KDG cyclone is 9.510.0 m/s, at the presence of which the cyclone achieves the best efficiency, i.e. 90.3±0.15%.

3. The comparison of modelling results (tangential air flow velocities) and experimental data has shown the average relative error of ±4.3%.

References

Altmeyer, S.; Mathieu, V.; Jullemier, S.; Contal, P.; Midoux, N.; Rode, S.; Leclers, J .P. 2004. Comparison of different models of cyclone prediction performanse for various operating conditions using a general software, *Chem. Eng. Prog.* 43: 511–522.
http://dx.doi.org/10.1016/S0255-2701(03)00079-5

Balan, S. A.; Burov, A. I.; Burov, A. A.; Serebrianskij, D. A. 2002. Apparatus with closed contours, in *Selection of Scientific articles «Ecology and Human health. Protection of water and atmospheric basins. Utiliation of waste»*. Energosteel-Xarkov, 320–325.

Baltrėnas, P.; Kvasauskas, M. 2005. Eksperimentiniai dalelių koncentracijų tyrimai taikant svorinį ir optinį metodus, *Journal of Environmental Engineering and Landscape Management* 13(2): 57–64.

Baltrėnas, P.; Morkūnienė, J.; Vaitiekūnas, P. 2008. Numerical simulation of solid particle dispersion in the air of Vilnius City, *Journal of Environmental Engineering and Landscape Management* 16(1): 15–22.
http://dx.doi.org/10.3846/1648-6897.2008.16.15-22

Bernardo, S.; Mori, M.; Peres, A. P.; Dionı´sio, R. P. 2006. 3-D computational fluid dynamics for gas and gas-particle flows in a cyclone with different inlet section angles, *Powder Technology* 162(2006): 190–200.
http://dx.doi.org/10.1016/j.powtec.2005.11.007

Boysan, F.; Ayers, W. H.; Swithenbank, J. A. 1982. A fundamental mathematical modeling approach to cyclone design, *Institution of Chemical Engineers* 60: 222–230.

Bradulienė, J.; Vasarevičius, S. 2010. Experimental investigation into reduction of gravel road dustiness using "safecote" solution and its mixture with $CaCl_2$, *Journal of Environmental Engineering and Landscape Management* 18(2): 145–153.

Cristea, E. D.; Malfa, E.; Coghe, A. 1996. 3-D numerical simulation and measurement of strongly swirling heavy dust-laden flow inside a cyclone separator, in *3rd International Symposium on Engineering Turbulence Modeling and Measurements*. Crete. Greece.

Derksen, J. J. 2003. Separation performance predictions of a Stairmand high efficiency cyclone, *AIChE Journal* 49: 1359–1371. http://dx.doi.org/10.1002/aic.690490603

Gimbun, J.; Chuah, T. G.; Fakhru'l-Razi, A.; Choong, T. S. Y. 2005. The influence of temperature and inlet velocity on cyclone pressure drop: A CFD study, *Chem. Eng. Prog.* 44: 7–12. http://dx.doi.org/10.1016/j.cep.2004.03.005

Gong, A. L.; Wang, L. Z. 2004. Numerical study of gas phase flow in cyclones with the repds, *Aero Technol.* 38: 506–512. http://dx.doi.org/10.1080/02786820490449548

Gujun, W.; Guogang, S.; Xiaohu, X.; Mingxian, S. 2008. Solids concentration simulation of different size particles in a cyclone separator, *Powder Technology* 183(2008): 94–104. http://dx.doi.org/10.1016/j.powtec.2007.11.019

Hashremi, S. B. 2006. A Mathematical model to compare the efficiency of cyclones, *Chem. Eng. Technol.* 29(12): 1444–1454. http://dx.doi.org/10.1002/ceat.200600217

Hoekstra, A. J.; Derksen, J. J. and Van Den Akker, H. E. A. 1999. An experimental and numerical study of turbulent swirling flow in gas cyclones, *Chem. Eng. Sci.* 54: 2055–2065. http://dx.doi.org/10.1016/S0009-2509(98)00373-X

Hoffmann, A. C; Stein, L. E. 2002. *Gas Cyclone and Swirl Tubes-Principles, Design and Operation*. Springer-Verlag, Berlin.

Hu, L. Y.; Zhou, L. X.; Zhang, J.; Shi, M. X. 2005. Studies on strongly swirling flows in the full space of volute cyclone separator, *AIChE Journal* 51(3): 740–749.
http://dx.doi.org/10.1002/aic.10354

Ingham, D. B.; Ma, L. 2002. Predicting the performance of air cyclones, *Int. J. Energy Res*. 26: 633–652.
http://dx.doi.org/10.1002/er.808

Jakštonienė, I.; Vaitiekūnas, P. 2009. Applying computational fluid dynamics modelling for investigating conical reverst-flow cyclone, *Mokslas – Lietuvos ateitis. Aplinkos apsaugos inžinerija* [Science – Future of Lithuania. Environmental Protection Engineering] 1(4): 51–55.

Kavaliauskas, A.; Vaitiekūnas, P. 2001. Modelling of Reynolds stresses in overflowing air stream in a square channel [Reinoldso įtempimų modeliavimas oro srautui aptekant kliūtį kvadratiniame kanale], *Energetika* (3): 38–43.

Kaya, F.; Karagoz, I. 2008. Performance analysis of numerical schemes in highly swirling turbulent flows in cyclones, *Current Science* 94(10): 1273–1278.

Meier, M.; Mori, M. 1999. Anisotropic behavior of the Reynolds stress in gas and gas – solid flows in cyclones, *Powder Technology* 101(1999): 108–119. http://dx.doi.org/10.1016/S0032-5910(98)00162-4

Morsi, S. A.; Alexander, A. J. 1972. An investigation of particle trajectories in twophase flow systems, *Journal of Fluid Mechanics* 55 (2):193–208. http://dx.doi.org/10.1017/S0022112072001806

Patankar, S. V. 1980. *Numerical Heat Transfer and Fluid Flow*. Hemisphere (McGraw-Hill), New York. 176 p.

Petraitis, E.; Vasarevičius, S. 2001. Kietųjų dalelių sklaidos atmosferoje skaitinis modeliavimas taikant „Varsa" ir „Phoenics" programas, *Journal of Environmental Engineering and Landscape Management* 9(1): 23–28.

Serebrianskij, D. A.; Novakovskij, J. V. 2009. Gas cleaning of dust in centrifugal filters, *Industrial Heat Engineering* 3.

Sommerfeld, M.; Ho, C. H. 2003. Numerical calculation of particle transport in turbulent wall bounded flows, *Powder Technology* 131: 1–6. http://dx.doi.org/10.1016/S0032-5910(02)00293-0

Spalding, D .B. 2002. *PHOENICS 3.5 VR CFD codes*. Available from internet: http://cham.co.uk/

Vaikasas, S. 2010. Mathematical modelling of sediment dynamics and their deposition in Lithuanian rivers and their deltas (case studies), *Journal of Environmental Engineering and Landscape Management* 18(3): 207–216. http://dx.doi.org/10.3846/jeelm.2010.24

Vaitiekūnas, P. 1998. *Konvekcinio pernešimo skaitinis modeliavimas*. Kaunas, Lietuvos energetikos institutas. 261 p.

Vaitiekunas, P.; Jakštonienė, I.; Serebrianskyy, D. 2010. Analysis of numerical modelling of turbulence in the multichannel cyclone, *Chemical and Process Engineering* 31(4): 635–645.

Vaitiekūnas, P.; Petkevicienė, J.; Markevicius, A. 2002. Twophase numerical model of heat transfer in a cooling pond, in *12th IHTC Grenoble*, August 18–23: 12.

Wang, B.; Xu, D. L.; Chu, K. W.; Yu, A. B. 2006. Numerical study of gas-solid flow in a cyclone separator, *Applied Mathematical Modelling* 30: 1326–1342. http://dx.doi.org/10.1016/j.apm.2006.03.011

Yakhot, V.; Orszag, S. A. 1986. Renormalization group analysis of turbulence. I. Basic theory, *J. Sci. Comput.* 1: 1–51. http://dx.doi.org/10.1007/BF01061452

Youngmin, Jo.; Chi, Y.; Madhumita, B. R. 1999. Development of a post cyclone to improve the efficiency of reverse flow cyclones, *Powder Technology* 113: 97–108.

Zhao, B.; Su, Y.; Zhang, J. 2006. Simulation of gas flow pattern and separation efficiency in cyclone with conventional single and spiral double inlet configu-ration, Trans IChemE. PA, *Chemical Engineering Research and Design* 84: 1158–1165. http://dx.doi.org/10.1205/cherd06040

Zhongli, Ji; Zhiyi, X.; Xiaolin, W.; Honghai, C.; Hongxiao, W. 2009. Experimental investigations on a cyclone separator performance at an extremely low particle concentration, *Powder Technology* 191: 254–259. http://dx.doi.org/10.1016/j.powtec.2008.10.015

Zhou, L. X.; Soo, S. L. 1990. Gas solid flow and collection of solids in a cyclone separator, *Powder Technology* 63(1): 45–53. http://dx.doi.org/10.1016/0032-5910(90)80006-K

ORO IR KIETŲJŲ DALELIŲ SRAUTO DAUGIAKANALIAME CIKLONE TYRIMAS

P. Baltrėnas, P. Vaitiekūnas, I. Jakštonienė, S. Konoverskytė

S a n t r a u k a

Nagrinėjama dujų ir kietųjų dalelių aerodinamika daugiakanaliame (trijų žiedų) išcentriniame ciklone-filtre (keturkanalis dulkių gaudytuvas – KDG). Srauto įtekėjimas tangentinis. Apžvelgti eksperimentiniai ir teoriniai procesų tokiuose ciklonuose, kuriuose susidaro ypač sudėtingas sūkurinis srautas, tyrimo darbai. Atliktas eksperimentinis tyrimas ir skaitinis oro srauto judėjimo KDG ciklone modeliavimas (ciklonas 0,72 m aukščio ir 0,50 m skersmens, cilindrinės dalies aukštis – 0,29 m, kūginės (dulkių rinktuvo) – 0,43 m, įtekėjimo angos plotas – 0,29×0,034 m²). Ciklono eksperimentiniams tyrimams naudota *Testo* 400 daugiafunkcis matuoklis, skirtas oro srauto greičiui matuoti daugiakanalio ciklono įtekėjimo ir ištekėjimo angose. Pateiktosios pernašos trimatės diferencialinės lygtys (Reinoldso) atvejo, kai turbulentinis srautas ciklono viduje nespūdusis, skaitiškai spręstos baigtinių tūrių metodu, taikant standartinį *k*-ε, ir RNG *k*-ε turbulencijos modelius. Remiantis tyrimų rezultatais, didžiausiasis ciklono su kvarcinio smėlio ir kvarcinio smėlio dulkių teršalais valymo efektyvumas siekė 85,8–90,4 %. Modeliavimo rezultatai, kai įtekėjimo greitis 6,27–10,78 m/s ir debitas – 0,111–0,190 m³/s, atitinkamai neblogai sutapo su eksperimentų duomenimis. Vidutinė santykinė paklaida siekė ±4,3 proc.

Reikšminiai žodžiai: ciklonas-filtras, kietosios dalelės, skaitinis modeliavimas, turbulentumas, vienfazis oro srautas, dvifazis srautas.

Pranas BALTRĖNAS. Dr Habil, Prof. and Head of Dept of Environmental Protection, Vilnius Gediminas Technical University (VGTU). Doctor Habil of Science (air pollution), Leningrad Civil Engineering Institute (Russia), 1989. Doctor of Science (air pollution) Ivanov Textile Institute (Russia), 1975. Employment: Professor (1990), Associate Professor (1985), senior lecturer (1975), Vilnius Civil Engineering Institute (VISI, now VGTU). Publications: author of 13 monographs, 24 study-guides, over 320 research papers and 67 inventions. Honorary awards and membership: prize-winner of the Republic of Lithuania (1994), a corresponding Member of the Ukrainian Academy of Technological Cybernetics, a full Member of International Academy of Ecology and Life Protection. Placements in Germany and Finland. Research interests: air pollution, pollutant properties, pollution control equipment and methods.

Petras VAITIEKŪNAS. Prof. Dr Habil of Dept of Environmental Protection, Vilnius Gediminas Technical University (VGTU). Doctor Habil of Science (energy and thermal engineering) Lithuanian Energy Institute, 1999. Doctor of Science Laboratory of Fluid Dynamics in Heat Exchangers Lithuanian Energy Institute, 1972. Employment: Professor (2002), Associate Professor (1997). Publications: author of 1 monograph, 3 educational books, over 230 research papers Membership: prize-winner of the Republic of Lithuania (2006), a corresponding Member of International Academy of Ecology and Life Protection. Research interests: hydrodynamics, convective heat and mass transfer and thermophysics, computational fluid dynamics, mathematical modeling of transfer processes in the environment.

Inga JAKŠTONIENĖ. Master PhD student, Dept of Environmental Protection, Vilnius Gediminas Technical University (VGTU). Master of Chemical Engineering, Engineer. Kaunas University of Technology, 2007, Faculty of Chemical Technology. Bachelor of Environmental Engineering, Environmental Engineering. Kaunas University of Technology, 2005, Faculty of Chemical Technology. Publications: author of 2 scientific publications. Research interests: protection of the atmosphere.

Simona KONOVERSKYTĖ. Master at the Department of Environmental Protection, Vilnius Gediminas Technical University (VGTU). Bachelor of Environmental Protection and Ecology. Šiauliai University 2006. Publications: author of 1 scientific publication. Research interests: protection of the atmosphere.